Evaluation of Liver Tumors Using Fluorine-18-Fluorodeoxyglucose PET: Characterization of Tumor and Assessment of Effect of Treatment

Shinichi Okazumi, Kaichi Isono, Kazuo Enomoto, Toshiyuki Kikuchi, Masahiko Ozaki, Hiroshi Yamamoto, Haruyuki Hayashi, Takehide Asano, and Munemasa Ryu

Second Department of Surgery, Chiba University School of Medicine, Chiba, Japan

To evaluate glucose metabolism in patients with tumors involving the liver, 35 patients with liver lesions had PET using ^{18}F-2-fluoro-2-deoxy-D-glucose (FDG). FDG (148 MBq) was injected and radioactivity of the tumor was scanned dynamically by PET. The rate constants (k_1, k_2, k_3, k_4) of FDG in a metabolic model were calculated. The results were compared to hexokinase activity in the excised tumor specimens. k_3 was found to reflect tumor hexokinase activity. When k_3 was used as an index (cut-off value: 0.025), it was possible to distinguish benign and malignant tumors. k_4 was significantly higher in hepatocellular carcinoma. By using k_3 and k_4 as indices, one could assess the degree of differentiation of hepatocellular carcinoma. After treatment, k_3 decreased according to the effectiveness of therapy and thus may be a useful index for quantitatively assessing tumor viability.

J Nucl Med 1992; 33:333–339

It is known that the rate of glucose metabolism is increased in malignant tumors (*1–3*) and this is regarded as an important indication of tumor proliferation. If this biological characteristic could be evaluated in vivo, useful information might be obtained regarding the characteristics of tumors and the effects of treatment.

In this study, ^{18}F-2-fluoro-2-deoxy-D-glucose (FDG) was used as a tracer of glucose metabolism and an analysis of glucose metabolism dynamics was performed in patients with tumors involving the liver with PET. FDG PET has been used mainly for neurologic studies (*4*) in which the uptake characteristics of FDG by malignant brain tumors have been reported (*5–7*). Although data on FDG uptake by liver tumors have been reported (*8,9*), no detailed analysis has yet been made. In this study, a detailed analysis of the glucose metabolism of liver tumors was performed to develop a method for assaying glycolytic enzymes in vivo and to determine the glycolytic characteristics of those tumors. We also attempted to distinguish between benign and malignant liver tumors and evaluate the effects of treatment.

Received May 31, 1991; revision accepted Jan. 10, 1992.

For reprints contact: Shinichi Okazumi, MD, Department of Surgery, Numazu City Hospital, 550 Harunoki Aza Higashishiiji Numazu, 410-03 Japan.

METHODS

Patients

Thirty-five patients with liver tumors, including 23 with primary liver cancer [20 hepatocellular carcinomas (HCC) and 3 cholangiocellular carcinomas (CCC)], 10 with metastatic liver cancer (five arising from the large bowel, two from the esophagus, two from the stomach, and one from the pancreas) and 2 with liver hemangioma. The patients were untreated and the tumor diameter was over 3 cm for all patients. Twelve individuals with normal livers and 10 patients with cirrhosis of the liver were also studied as controls.

Tracer Synthesis and Instrumentation

Fluorine-18 was manufactured from ^{20}Ne(d, α)^{18}F with a small "CYPRIS" cyclotron (Sumitomo Heavy Industries). FDG was synthesized by the acetylhypofluorite method with a "CUPID" automatic tracer. The preparation was tested in accordance with the standards of the cyclotron committee of Chiba University Hospital. The radiochemical purity of FDG was more than 95%. PET images were obtained on a HEADTOME III (Shimazu Works) scanner. A ramp filter and a Butterworth filter (cut-off frequency: 8 mm^{-1}, order 3) were used for image reconstruction, resulting in an in-plane spatial resolution of 10.5 mm (FWHM) in which the resolution in the z-axis direction was 16.5 mm.

PET Scanning

Once patients were positioned, transmission scans were obtained with a ^{68}Ge ring. After cannulation of the peripheral vein and brachial artery, FDG (148 MBq) was administered intravenously for about 2 min. Upon injection to 60 min after administration, arterial blood samples were collected successively (15-sec interval × 9, 30-sec interval × 4, 1-min interval × 4, 2-min interval × 2, 3-min interval × 1, 5-min interval × 3, and 10-min interval × 3). In addition, dynamic scanning of the tumor was performed (2-min scans × 5 and 5-min scans × 10). After the arterial blood samples were centrifuged, radioactivity in the plasma (Cp) was measured with a well counter. Changes of radioactivity in the tumor (Ci) were measured over time from the PET images. In these measurements, a region of interest (9 pixels) was designated at the site of maximum accumulation in the tumor and the mean radioactivity (cps/ml) was determined. No correction was made for the tumor-blood volume.

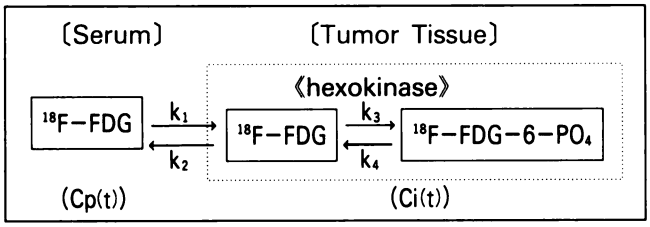

FIGURE 1. Compartment model of [^{18}F]FDG. k_1, k_2, k_3, k_4: rate constants.

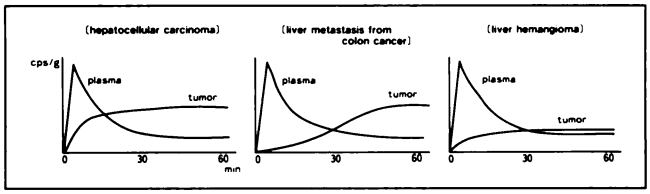

FIGURE 2. Time-activity curve of plasma and tumor after the injection of FDG.

Data Analysis

The following analysis was made using a metabolic model designed for FDG in brain tissue by Phelps et al. (*10*) (Fig. 1). The rate constants used were: k_1, transfer from blood into tissue; k_2, transfer from tissue into blood; k_3, phosphorylation by hexokinase; and k_4, dephosphorylation by G-6-phosphatase.

Using the successive values of Cp and Ci obtained as mentioned above, we calculated the rate constants k_1 to k_4 by the non-linear least squares method. Calculations were performed using the NUMPAC program, and the algorithm of the least squares method was determined using a HITAC-M680 program and quasi-Newtonian methods.

Measurement of Tumor Hexokinase Activity

To confirm the ability of this model to reflect metabolism in the liver, hexokinase activity in tumor tissue was measured in accordance with the method of Monakhov et al (*11*). This procedure was performed on seven patients with hepatocellular carcinoma, two patients with metastatic liver cancer and one patient with liver hemangioma in whom the excised specimens could be examined. After excision, the specimens were cut into transverse sections in accordance with the preoperative PET slices. The tissue specimen for analysis was obtained immediately after excision from the area corresponding to the ROI in the preoperative PET image.

RESULTS

PET Imaging

In the non-cancerous portion, both normal and cirrhotic livers showed marked accumulation of ^{18}FDG throughout the early period after intravenous injection of the tracer. Accumulation subsequently decreased rapidly with time and a steady-state was reached after 60 min (Fig. 2). FDG accumulation varied in all liver tumors during the early period after injection of the tracer, but after 60 min it reached a steady-state irrespective of tumor vascularity (Fig. 3).

Hepatocellular carcinomas were divided into three types depending on the pattern of accumulation 60 min after the injection of FDG. Type 1 lesions showed greater accumulation after 60 min compared with the surrounding liver (Fig. 3A). Type 2 lesions showed nearly the same degree of accumulation as the surrounding liver tissue (Fig. 3B), and type 3 tumors showed less accumulation than the surrounding liver tissue (Fig. 3C). Type 1 tumors were found in 11 patients (55%), type 2 tumors in 6 patients (30%), and type 3 tumors in 3 patients (15%).

Cholangiocellular carcinoma (Fig. 3D) and metastatic liver cancer (Fig. 3E) showed less accumulation than the surrounding liver tissue in the early period, but showed greater accumulation after 60 min (corresponding to type 1 HCC).

The liver hemangioma (Fig. 3F) showed patchy accumulation in the early period, but this gradually became uniform and equal to that of the surrounding liver tissue after 60 min (corresponding to type 2 HCC).

Rate Constants (k_1 to k_4)

Rate constants for FDG transport into each liver tumor were calculated (Fig. 4). k_1 values varied somewhat but the

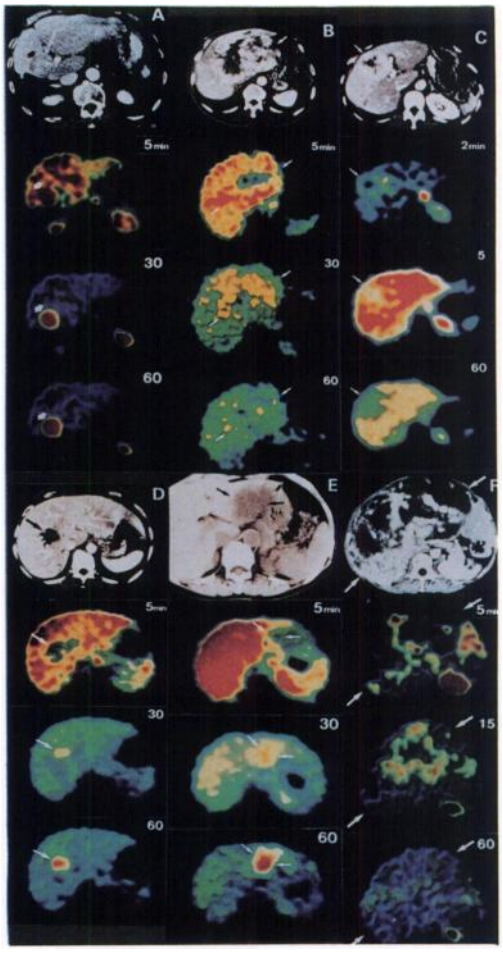

FIGURE 3. FDG PET images of liver tumors. (A) hepatocellular carcinoma (type 1), (B) hepatocellular carcinoma (type 2), (C) hepatocellular carcinoma (type 3), (D) cholangiocellular carcinoma, (E) liver metastasis from colon cancer, and (F) liver hemangioma. Arrows indicate the tumor. Top image is enhanced CT (A, B, C, D, F) or plain CT (E). The middle and bottom images are dynamic PET using FDG.

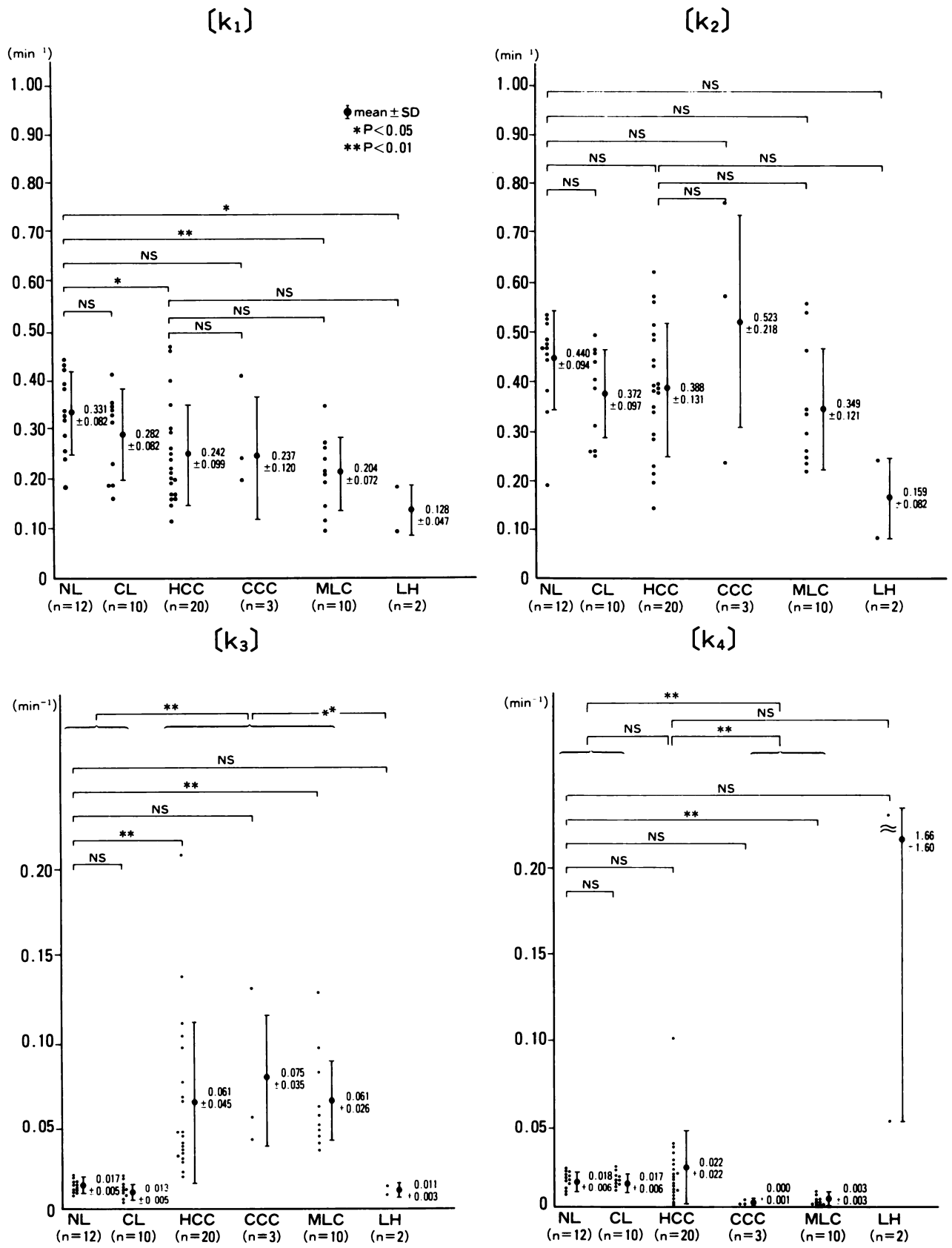

FIGURE 4. The values of rate constants k_1 to k_4 in liver tumors and in the non-cancerous portion. NL = normal liver, CL = cirrhotic liver, HCC = hepatocellular carcinoma, CCC = cholangiocellular carcinoma, MLC = metastatic liver cancer, and LH = liver hemangioma.

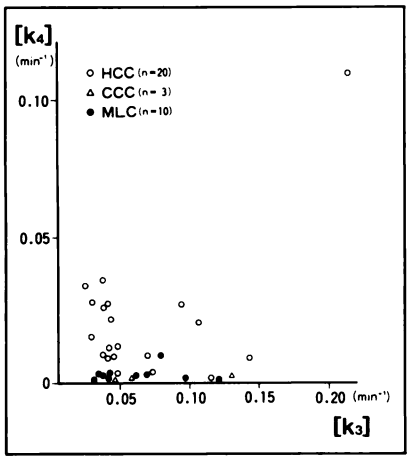

FIGURE 5. The relationship between k_3 and k_4 values in each liver cancer.

mean value was similar for HCC, CCC and metastatic liver cancer (MLC), and the lowest value was obtained for liver hemangioma (LH). There were no significant differences in k_1 values among these types of tumors, while the values for normal liver tissue (NL) were significantly higher than those for HCC, MLC and LH (i.e., the glucose transfer rate from the blood to the tissue was slower in the tumors). Cirrhotic liver (CL) tissue had a similar k_1 value to NL.

Tumor k_2 values showed a similar pattern to the k_1 values, but there were no significant differences in k_2 between NL and the tumors.

The k_3 value was 0.061 ± 0.046 (min^{-1}) for HCC, 0.075 ± 0.035 for CCC, 0.061 ± 0.026 for MLC, 0.011 ± 0.003 for LH, 0.017 ± 0.005 for NL, and 0.013 ± 0.005 for CL. There were no significant differences in k_3 between NL and CL. HCC, CCC and MLC also showed no significant differences, but the malignant tumors had significantly higher values than the benign tumors and non-tumor liver tissue (NL + CL). Furthermore, at $k_3 \geqq 0.025$, 100% of the tissues were malignant, while for $k_3 < 0.025$ it was found that 92.3% were benign. The two malignant tumors with a k_3 value < 0.025 were both HCC (k_3: 0.0178, 0.0213).

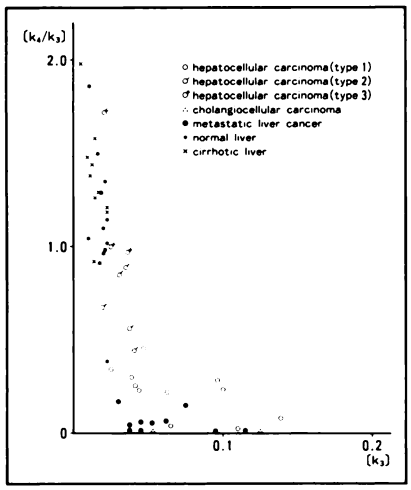

FIGURE 5. The relationship between k_3 and k_4 values in each liver cancer.

The k_4 values were nearly zero for CCC (k_4: 0.000 ± 0.001) and MLC (k_4: 0.003 ± 0.003), whereas HCC showed a wide distribution of k_4 values (k_4: 0.022 ± 0.022). Normal liver (k_4: 0.018 ± 0.006) and cirrhotic liver (k_4: 0.017 ± 0.006) had similar k_4 values. The k_4 values for HCC or for the surrounding liver tissue (NL + CL) were significantly higher than those for non-HCC liver cancer.

When the relationship between k_3 and k_4 values was assessed for malignant tumors (Fig. 5), k_4 was nearly zero in CCC and MLC, irrespective of the value of k_3, whereas most HCCs with a low k_3 showed a high k_4 value. The k_4/k_3 ratio was obtained for each type of liver cancer, and its relation to k_3 was studied (Fig. 6). In CCC and MLC, the k_4/k_3 ratio was nearly zero, irrespective of the value of k_3, whereas for HCC a low k_3 value was associated with a high k_4/k_3 ratio (similar to that for the surrounding liver tissue). Type 1 HCC had higher k_3 values and lower k_4/k_3 ratios, type 2 HCC had similar k_4/k_3 ratios to the surrounding liver tissues, and type 3 HCC had especially high k_4/k_3 ratios. This showed that the differences in FDG accumulation on PET images in HCC were related to the k_4/k_3 ratio (i.e., higher accumulation of FDG (type 1) corresponded to a lower ratio and lower accumulation (type 3) corresponded to a higher ratio). Thus, liver cancer had a significantly higher k_3 value than normal liver tissue. Also, some HCCs had similar k_4 values to normal liver.

This characteristic was not found for CCC and MLC, while in HCC the k_4/k_3 ratio was related to the differences in FDG accumulation on PET images. No significant difference in k_1 or k_2 values was noted between type 1 HCC and types 2 or 3.

Effects of Treatment

The k_3 value was considered to have the closest relationship to tumor glucose metabolism. Thus changes of this constant after treatment of liver cancer were studied.

Case 1 was a patient with HCC who underwent transcatheter arterial embolization (TAE). After TAE, FDG accumulated in the tumor periphery, corresponding to the deposition of lipiodol on CT scans, and the k_3 value at this site was 0.047. On the other hand, the tumor center showed very little accumulation and the k_3 value was only 0.017. Examination of the excised specimen showed that the tumor periphery was viable, while the central zone had undergone necrosis.

Patient 2 had HCC, and the PET images obtained before and after TAE are shown in Figure 7. Before TAE, accumulation of FDG was noted in the tumor and the k_3 value was 0.042. After TAE, the deposition of lipiodol was noted in the tumor and the tumor diameter was nearly unchanged, but FDG no longer accumulated and the k_3 value was decreased to 0.024. Examination of the excised specimen showed complete necrosis of the tumor. The decrease in the k_3 value was statistically significant ($p < 0.01$). This decrease was attributed to a loss of tumor hexokinase activity after treatment.

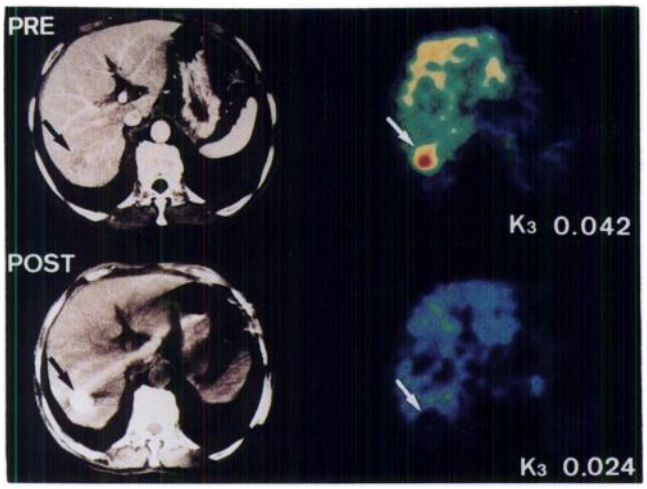

FIGURE 7. Patient 2 had HCC and underwent TAE. Arrows indicate tumor. (Top) Images before TAE and (bottom) images after TAE. (Left) Enhanced CT images and (right) FDG PET images 60 min after injection.

Measurement of Hexokinase Activity

In 10 patients for whom excised specimens could be examined, the relationship between hexokinase activity (units/g tissue) and the k_3 value obtained preoperatively was assessed (Fig. 8). Since the k_3 value reflects the total hexokinase activity per unit volume of tumor tissue, this activity was also expressed per unit volume. Because the excised specimens were assayed, there is a possibility that the activity was slightly decreased by handling, but a significant correlation with k_3 was still noted ($p < 0.05$).

DISCUSSION

Glucose metabolism is increased in malignant tumors (*1–3*), and hexokinase activity (which phosphorylates glucose in the glycolytic pathway) correlates with tumor proliferative activity (*12–14*). In this study, we used PET and [^{18}F]FDG to examine the glucose metabolism of liver tumors. This analog of glucose enters the cell and is phosphorylated by hexokinase; but since it is not a substrate of phosphohexose isomerase (the enzyme involved in the next step of the glycolytic pathway), it accumulates intracellularly as FDG-6-PO_4.

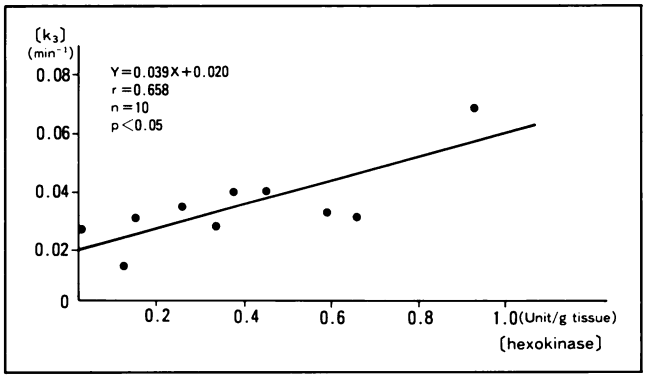

FIGURE 8. The relationship between k_3 and the hexokinase activity. The values of k_3 of liver tumors are significantly related to their hexokinase activities.

In this study, we used the metabolic model of Phelps et al., which was developed for the brain and is a modification of Sokoloff's model (*15*). Since the tumor k_3 value showed a significant correlation with the measured hexokinase activity, it appears reasonable to use this model in the analysis of liver tumors.

It should be remembered that two systems of blood supply (the portal vein and the hepatic artery) are present in the liver. It is thus better to use data from these two systems as the input function, but it is clinically difficult to measure them separately in patients during PET imaging. Also, after intravenous injection, FDG spreads rapidly through the blood system. We therefore used the data from brachial arterial blood as the approximate value of the input function. Previous studies of liver-tumor blood supply have shown that these lesions are supplied largely by the hepatic artery (*16*), making it reasonable to use brachial artery data as the input function.

Our analysis showed that k_1 (the rate of glucose inflow from the plasma into the cells) was lower for the tumors than for the surrounding liver tissue. A similar finding has also been reported for brain tumors (*17*), but the clinical significance is unknown at present.

The rate constant k_3 (phosphorylation by hexokinase) was significantly increased in malignant tumors, and we were able to identify benign and malignant lesions by taking a cut-off value of 0.025 for this constant. This result agrees with previous reports (*18,19*) showing that hexokinase activity is increased in malignant tumors. Hexokinase activity is also said to correlate with the proliferative activity of a tumor (*14,20*), so the k_3 value may perhaps reflect tumor aggressiveness. However, since clinical practice offers few chances to observe the natural course of a tumor and it is difficult to calculate the doubling time, this point requires further study.

k_4 is the rate constant for dephosphorylation by glucose-6-phosphatase, an enzyme present specifically in the liver and kidney (*21,22*), that is rarely detected in other tissues or tumors. We found a k_4 value of nearly zero in CCC and MLC, while about 45% of HCC showed similar k_4 values to the surrounding liver tissue. From this result, some HCCs may partly retain the properties of normal liver and the degree of this retention may be indicated by the k_4 value. Thus, k_4 may be a useful diagnostic index not only to distinguish HCC from other liver tumors but also to indicate the degree of differentiation of HCC.

The PET images taken 60 min after injection showed three patterns of FDG accumulation in liver cancers. Higher accumulation than the surrounding liver tissue, the so-called hot nodule, accounted for 55% of HCC (type 1) and for all cases of CCC and MLC. Similar or lower accumulation than the surrounding liver was found only in HCC (types 2 and 3). These differences could be explained by the k_3 and k_4 values of tumors (i.e., tumors

with a higher FDG accumulation had k_4 values lower than their k_3 values irrespective of the type of liver cancer, particularly the k_4 of CCC or MLC, which was nearly zero, whereas tumors with similar or lower accumulation than the surrounding liver tissue had a k_4 value close to or higher than their k_3 value). There was no significant difference in k_1 among types 1 and 2 or 3, so it was assumed that the differences of FDG accumulation seen in HCC were not due to variations in the transfer of FDG from blood to tissue but were due to differences in the relationship between phosphorylation and dephosphorylation of FDG.

In this way, it was proved that FDG accumulation in some HCCs was modified by a high k_4, and that these appeared as low accumulation images on PET, even when their k_3 values were of a malignant level. To differentiate benign and malignant lesions in such cases, it was thought necessary to calculate the k_3 and k_4 values by a dynamic study.

The graphical method of dynamic study (*23,24*) can be used to calculate the metabolic rate of glucose from the slope of the graph ($[k_1 \times k_3]/[k_2 + k_3]$). It is a useful method for evaluating many kinds of tumors and the slope can be used as successfully as k_3 most of the time. However, the graphical method was devised for the analysis of the brain where k_4 was neglected. When the method is applied to types 2 or 3 HCC, the value $[k_1 \times k_3]/[k_2 + k_3]$ obtained from the slope is inadequate and lower than that from the compartment model data $[k_1 \times k_3]/[k_2 + k_3]$. Therefore, some HCCs should be evaluated by the compartment model because of a high k_4 value.

In experimental studies on liver cancer, hexokinase activity reportedly increases during carcinogenesis (*20*) and G-6-Pase activity decreases finally to zero (*21,25*). Therefore enzymatic assessment of tumors with k_3 and k_4 as the indices as well as assessment of the degree of differentiation of HCC by glucose metabolism are suggested. We found that many HCCs with high k_4 values had low k_3 values, and that those with low k_4 values had high k_3 values. The k_4/k_3 ratio varied from tumors that were similar to normal or cirrhotic liver tissue (types 2 and 3) to lesions showing a similar ratio to CCC and MLC (type 1) (Fig. 1). As the k_3 value becomes higher, tumor tissue further departs from normal liver tissue, and as the k_4/k_3 ratio becomes higher it moves closer to normal liver tissue. This suggests that the degree of differentiation of HCC may be assessed using k_3 and k_4 as the indices.

As to the effect of TAE or radiotherapy on liver tumors, US, CT, and MRI are generally used to assess any reduction in size or changes of the internal structure. However, in some liver tumors, the diameter does not change and only the internal structure changes. In addition, lipiodol deposits can make the evaluation more difficult. We found that by using k_3 as an index, a quantitative evaluation was possible irrespective of the change in tumor diameter (or the lack thereof), even after lipiodol deposition. Glucose is generally the main source of energy for a tumor, and nucleic acids are synthesized via the pentose shunt from glucose-6-phosphate, thus hexokinase is considered to be an important enzyme in tumor proliferation. When tumor cells are destroyed by various treatments, the hexokinase activity decreases correspondingly and enzymatic evaluation of tumor viability should be possible by measuring the activity in vivo by FDG PET. In contrast to image diagnosis, the quantitative evaluation of viability by glucose metabolism is not influenced by tumor size, morphology, vascularity, or lipiodol deposition.

The subjects of this study were restricted to those having tumors of 3 cm or more in diameter because of the limited resolution of the PET scanner, but with future technical improvements it should be possible to analyze smaller liver tumors.

CONCLUSION

FDG PET was used to evaluate glucose metabolism in liver tumors. We used the MULTI-compartment model of Phelps et al. to obtain the k_1 to k_4 rate constants for FDG transport. The k_3 value was considered to reflect hexokinase activity, a glycolytic phosphorylating enzyme that increases in malignant tumors. Distinguishing between benign and malignant lesions was possible by taking a cut-off value of 0.025 for k_3. k_4, the dephosphorylation rate constant values of CCC or MLC, was nearly zero, while some HCCs showed similar k_4 values to the surrounding liver tissue. k_4 may also be a useful diagnostic index not only to distinguish HCC from other liver tumors but also to indicate the degree of retention of properties of normal liver in some HCCs. It is suggested that the degree of differentiation of HCC can be assessed using k_3 and k_4 as the indices by the glucose metabolism. For the effect on treatment, a quantitative evaluation of tumor viability by glucose metabolism was considered to be possible by using k_3 as an index.

REFERENCES

1. Sweeney MJ, Ashmore J, Morris HP, Weber G. Comparative biochemistry of hepatomas. IV. Isotope studies of glucose and fructose metabolism in liver tumors of different growth rates. *Cancer Res* 1963;23:995–1002.
2. Lo C, Cristofalo VJ, Morris HP, Weinhouse S. Studies on respiration and glycolysis in transplanted hepatic tumors of the rat. *Cancer Res* 1968;28:1–10.
3. Burk D, Woods M, Hunter J. On the significance of glucolysis for cancer growth, with special reference to Morris rat hepatomas. *J Natl Cancer Inst* 1967;38:839–863.
4. Wienhard K, Pawlik G, Hertholz K, Wagner R, Heiss W-D. Estimation of local cerebral glucose utilization by positron emission tomography of [^{18}F] 2-fluoro-2-deoxy-D-glucose: a critical appraisal of optimization procedures. *J Cereb Blood Flow Metab* 1985;5:115–125.
5. Francavilla TL, Miletich RS, Chiro GD, Patronas NJ, Rizzoli HV, Wright DC. Positron emission tomography in the detection of malignant degeneration of low-grade gliomas. *Neurosurg* 1989;24:1–5.
6. Chiro GD: Positron emission tomography using [^{18}F]fluorodeoxyglucose in brain tumors: A powerful diagnostic and prognostic tool. *Invest Radiol* 1987;22:360–371.
7. Alavi JB, Alavi A, Chawluk J, et al. Positron emission tomography in

patients with glioma. *Cancer* 1988;62:1074–1078.
8. Yonekura Yoshihisa ABE, Benua RS, Brill AB, et al. Increased accumulation of 2-deoxy-2[^{18}F]fluoro-D-glucose in liver metastases from colon cancer. *J Nucl Med* 1982;23:1133–1137.
9. Fukuda H, Matsuzawa T, Abe Y, et al. Experimental study for cancer diagnosis with positron labeled fluorinated flucose analogs: [^{18}F]-2-fluoro-2-deoxy-D-mannose: a new tracer for cancer detection. *Eur J Nucl Med* 1982;7:294–297.
10. Phelps ME, Huang SC, Hoffman EJ, Selin C, Sokoloff L, Kuhl DE. Tomographic measurements of local cerebral glucose metabolic rate in humans with [^{18}F]2-fluoro-2-deoxy-D-glucose: validation of method. *Ann Neurol* 1979;6:371–388.
11. Monakhov NK, Neistadt EL, Shaviovlkii MM, Shvartsman AL, Neifakh SA. Physicochemical properties and isoenzyme composition of hexokinase from normal and malignant human tissues. *J Natl Cancer Inst* 1978;61:27–34.
12. Bustamante E, Morris HP, Pedersen PL. Energy metabolism of tumor cells. *J Biol Chem* 1981;256:8699–8704.
13. Knox WE, Jamdar SC, Davis PA. Hexokinase, differentiation and growth rate of transplanted rat tumors. *Cancer Res* 1970;30:2240–2244.
14. Weinhouse S. Glycolysis, respiration, and enzyme deletions in slow-growing hepatic tumors. *Gann Monogr* 1966;1:99–115.
15. Sokoloff L, Reivich M, Kennedy C, et al. The [^{14}C]deoxyglucose method for the measurement of local cerebral glucose utilization: theory, procedure, and normal values in the conscious and anesthetized albino rat. *J Neurochem* 1977;28:897–916.
16. Breedis C, Young G. The blood supply of neoplasms in the liver. *Am J Pathol* 1954;30:969–985.
17. Herholz K, Ziffling P, Staffen W, et al. Uncoupling of hexose transport and phosphorylation in human gliomas demonstrated by PET. *Eur J Cancer Clin Oncol* 1988;24:1139–1150.
18. Criss WE. A review of isoenzymes in cancer. *Cancer Res* 1971;31:1523–1542.
19. Weber G, Lui S, Takeda E, Denton JE. Enzymology of human colon tumors. *Life Sci* 1980;27:793–799.
20. Sharma RM, Sharma C, Donnelly AJ, Morris HP, Weinhouse S. Glucose-ATP phosphotransferases during hepatocarcinogeneses. *Cancer Res* 1965;25:193–199.
21. Weber G, Cantero A. Glucose-6-phosphatase activity in normal, precancerous, and neoplastic tissues. *Cancer Res* 1955;15:105–108.
22. Gallagher BM, Fowler JS, Gutterson NI, MacGregor RR, Wan CN, Wolf AP. Metabolic trapping as a principle of radiopharmaceutical design: some factors responsible for the biodistribution of [^{18}F]2-deoxy-2-fluoro-D-glucose. *J Nucl Med* 1978;19:1154–1161.
23. Patlak C, Blasberg RG, Fenstermacher JD. Graphical evaluation of blood-to-brain transfer constants from multiple uptake data. *J Cereb Blood Flow Metab* 1983;3:1–7.
24. Strauss LG, Clorius JH, Schlag P, et al. Recurrence of colorectal tumors: PET evaluation. *Radiology* 1989;170:329–332.
25. Weber G, Morris HP, Love WC, Ashmore J. Comparative biochemistry of hepatomas. II. Isotope studies of carbohydrate metabolism in Morris hepatoma 5123. *Cancer Res* 1961;21:1406–1411.

EDITORIAL

Quantitating Tumor Glucose Metabolism with FDG and PET

The glucose analog 2-[^{18}F]fluoro-2-deoxy-D-glucose (FDG) was first utilized with positron emission tomography (PET) in humans to quantify cerebral glucose metabolism (*1–3*), based on a tracer kinetic method initially developed for autoradiographic rat studies with ^{14}C-deoxyglucose by Sokoloff et al. (*4*). The method has been extended, with appropriate modifications, to other organ systems, including the heart (*5*). Because of the high glycolytic rate of many malignancies, qualitative and quantitative PET FDG imaging evaluations of tumors of the central nervous system (CNS) and other organ systems have demonstrated the potential utility of the method to detect the presence of malignant tissue and to quantify changes in tumor glycolysis during and after treatment (*6*). While reported quantitative PET FDG tumor studies during and after treatment are limited in number, most of these investigations have concerned radiotherapy, although some results with chemotherapy have also been reported (*7–12*). The majority of quantitative PET FDG tumor studies, other than those of astrocytomas (*13, 14*), have been based on nonkinetic evaluations of relative tumor FDG uptake, compared either to normal tissue or to injected dose per body weight (*6,7,15*).

Following facilitated diffusion from plasma to tissue, FDG is phosphorylated by hexokinase and trapped intracellularly as FDG-6-PO_4 (*2,4,16,17*), with, for most tissues, a very slow rate of dephosphorylation. Therefore, the 511 keV photons resulting from annihilation of the positron emitted by ^{18}F originate both from FDG distributed between plasma and tissue, and from FDG-6-PO_4 within cells. After about 40 min following intravenous injection of FDG, the majority of the ^{18}F label in the brain, heart, and most tumors originates from intracellular FDG-6-PO_4. In tissues with low rates of glucose-6-phosphatase mediated dephosphorylation, the accumulated amount of FDG-6-PO_4 is proportional to the glycolytic rate. Since by 40 min the majority of tissue activity is in the form of FDG-6-PO_4, images of total ^{18}F activity represent relative rates of glycolysis. This approximation is appropriate over a wide range of glycolytic rates, although it is less accurate at very low glycolytic rates.

One may therefore analyze PET FDG tumor studies on three levels: (1) qualitative inspection of static images, taken 40 min after injection, for identification of high local activities characteristic of aggressive tumors; (2) nonkinetic quantitative analyses of relative lesion activity concentration compared to injected dose per body weight or region of interest ratio methods; and (3) kinetic evaluations of tumor glucose metabolic characteristics, utilizing either the closed-form solution for the FDG model (Equation 2 below) and a priori estimates of model parameters (i.e., rate constants) with images obtained at a single time (the autoradiographic method) or employing a dynamic acquisition sequence and directly estimating model rate constants with nonlinear regression (Equation 1 below) (MR, in units of μmol/100 g/min) (*2–4*).

The kinetic methods then produce estimates of the tissue glucose meta-

Received Dec. 10, 1991; accepted Dec. 11, 1991.
For reprints contact: Randall A. Hawkins, MD, PhD, Division of Nuclear Medicine and Biophysics, Department of Radiological Sciences, UCLA School of Medicine, Los Angeles, CA 90024.